An integrated metabolomic and proteomic study of toxic effects of Benzo[a]pyrene on gills of the pearl oyster Pinctada ....

Article *in* Ecotoxicology and Environmental Safety · March 2018

DOI: 10.1016/j.ecoenv.2018.03.040

CITATIONS
0

READS
51

4 authors, including:

Hao Chen
Hainan University
6 PUBLICATIONS **29** CITATIONS
SEE PROFILE

Xiao-Ping Diao
Hainan University
35 PUBLICATIONS **200** CITATIONS
SEE PROFILE

Hailong Zhou
Hainan University
31 PUBLICATIONS **185** CITATIONS
SEE PROFILE

Ecotoxicology and Environmental Safety 156 (2018) 330–336

Contents lists available at ScienceDirect

Ecotoxicology and Environmental Safety

journal homepage: www.elsevier.com/locate/ecoenv

An integrated metabolomic and proteomic study of toxic effects of Benzo[a]pyrene on gills of the pearl oyster *Pinctada martensii*

Hao Chen[a,b], Xiaoping Diao[a,b,*], Haihua Wang[a,b], Hailong Zhou[a,b,*]

[a] State Key Laboratory of Marine Resource Utilization in South China Sea, Hainan University, Haikou 570228, China
[b] Institute of Tropical Agriculture and Forestry, Hainan University, Haikou 570228, China

ARTICLE INFO

Keywords:
Pinctada martensii
Benzo[a]pyrene
Biomarker
Metabolomic
Proteomic

ABSTRACT

Benzo[a]pyrene (BaP) is one of the most important polycyclic aromatic hydrocarbons (PAHs), which are widely present in the marine environment. Because of its teratogenic, mutagenic, and carcinogenic effects on various organisms, the toxicity of BaP is of great concern. In this study, we focused on the toxic effects of BaP (1 μg/L and 10 μg/L) on gills of the pearl oyster *Pinctada martensii* using combined metabolomic and proteomic approaches. At the metabolome level, the high concentration of BaP mainly caused abnormal energy metabolism, osmotic regulation and immune response marked by significantly altered metabolites in gills. At the proteome level, both concentrations of BaP mainly induced signal transduction, transcription regulation, cell growth, stress response, and energy metabolism. Overall, the research demonstrated that the combination of proteomic and metabolomic approaches could provide a significant way to elucidate toxic effects of BaP on *P. martensii*.

1. Introduction

Polycyclic aromatic hydrocarbons (PAHs) are widespread, persistent, bioaccumulative and ecologically toxic environmental pollutants. Benzo[a]pyrene (BaP) is a prominent member of the PAHs and is of vital concern due to its severe mutagenic, cytotoxic, teratogenic and carcinogenic effects (Tung et al., 2014; Uno et al., 2014; Zena et al., 2015). BaP is produced by the incomplete combustion of organic matter, and it has a strong affinity for sediment in the aquatic environment (Phillips, 1999; Williams and Hubberstey, 2014). Once BaP is metabolized by organisms, it may become a mutagenic agent in polluted environments (Wills et al., 2010). Several toxic effects of BaP on fish (Zhao et al., 2013; Corrales et al., 2014; Santacroce et al., 2015) and invertebrates (Rust et al., 2004; Liu et al., 2014a) have been reported. Previous studies have investigated concentrations of BaP in the different marine environment, ranging from 0.155 to 31.000 ng/L (Valavanidis et al., 2008; Qiu et al., 2009; Liu et al., 2014b).

The traditional biological approaches mainly focus on the detection of specific biological responses such as specific expressed genes or enzymes activity (Braz-Mota et al., 2015; Chivittz et al., 2016). However, a few established biomarkers have sensitivity and specificity for environmental contaminants stressors (Campos et al., 2012). With the rapid progress of "-omic" approaches, proteomics, metabolomics, transcriptomics and genomics have been widely applied in the study of environmental toxicology (Viant et al., 2003; Van Hummelen and Sasaki, 2010; Karim et al., 2011; Slattery et al., 2012). These omics are capable of discovering wider ranges of biomarkers at the molecular level. Metabolomics is research into the global changes of low molecular weight metabolites (< 1000 Da) in organisms. Metabolomics can reflect the mechanism of metabolic reactions induced by contaminants through comparing the profiles of metabolomes in organisms (Tikunov et al., 2010; Wu and Wang, 2010; Cappello et al., 2016a). Similar to metabolomics, proteomics is another efficient method that can be used to identify differential proteomes at the cell, tissue, and organ levels under different external stresses (Costa et al., 2010; Maria et al., 2013; Tomanek, 2014). Both metabolomics and proteomics are usually used to identify the abnormal changes in proteins and metabolic pathways induced by various environmental stressors (Wu et al., 2013a; Ji et al., 2016; Yu et al., 2016). Therefore, when combined, the approaches could be able to illustrate the toxic mechanisms of contaminants.

The pearl oyster *Pinctada martensii*, a vital bivalve species for producing artificial pearls, is widely distributed in subtropical and tropical oceans (Shi et al., 2013). *P. martensii* can be used as a new indicator organism for marine pollution due to its filter-feeding habitation and low metabolic rate (Du et al., 2015). Gills are the main target organs for the accumulation of pollutants in marine bivalve invertebrates (Panfoli et al., 2000; Ciacci et al., 2012; D'Agata et al., 2014; Azevedo et al., 2015). In this work, we selected the gills of *P. martensii* as the target organ, and ^{1}H NMR-based metabolomics with 2-DE-based proteomics to investigate the toxic effects of BaP.

* Corresponding authors at: Institute of Tropical Agriculture and Forestry, Hainan University, Haikou 570228, China.
E-mail addresses: chenhao.4788@hotmail.com (H. Chen), diaoxip@hainu.edu.cn (X. Diao), wanghaihua75@139.com (H. Wang), zhouhl@hainu.edu.cn (H. Zhou).

https://doi.org/10.1016/j.ecoenv.2018.03.040
Received 21 July 2017; Received in revised form 11 March 2018; Accepted 13 March 2018

2. Materials and methods

2.1. Experimental design and sample collection

Adult and healthy *P. martensii* (aged 2 years, 6.78 ± 0.35 cm) were collected from a site in the harbor (Lingshui, Hainan, China) in spring. The pearl oysters were acclimatized in aerated sand-filtered seawater (pH 8.2 ± 0.1; salinity 32‰) for 3 days in the laboratory, and fed with the marine microalgae *Tetraselmis chui* at a ration of 2% of tissue per dry weight daily. In exposure periods, these animals (30 per 40 L aquarium) were exposed to seawater, seawater with 0.001% acetone (v/v), low-dose BaP (1 μg/L) and high-dose BaP (10 μg/L) for 7 days. The concentrations of BaP were designed according to a pre-experiment and other reports (Zhang et al., 2004; Tian et al., 2015). They were fasted, and the seawater was renewed once every day during exposure periods. After exposure for 7 days, the gills of 12 individuals from each group were quickly dissected and shock-frozen in liquid nitrogen until investigation. For the metabolomics experiment, 12 biological replicates were used in each treatment. For the proteomics experiment, each treatment consisted of 3 biological replicates (4 oyster individuals were pooled into 1 sample).

2.2. Metabolomics analysis of P. martensii gills

Polar metabolites in gills of *P. martensii* were extracted by using a modified protocol (Lin et al., 2007; Wu et al., 2008). Approximately 100 mg of gills were homogenized and extracted in a solvent system of methanol/chloroform/water (400 μL: 200 μL: 85 μL). The extracts were subsequently dissolved in 600 μL of phosphate buffer (100 mM NaH_2PO_4 and Na_2HPO_4 with 0.5 mM sodium 3-trimethlysilyl-2, 2, 3, 3-d_4 propionate (TSP), pH 7.0) in D_2O. The mixture was vortexed and centrifuged at 3000 g for 5 min at 4 °C. The total volume of 550 μL supernatant substance was pipetted into a 5 mm NMR tube for NMR analysis.

Extracted metabolites were analyzed on a Bruker AV 500 NMR spectrometer as described previously (Zhang et al., 2011a). One-dimensional (1D) spectra were acquired using an 11.9 μs pulse, 0.1 s mixing time, and 3.0 s relaxation delay with a standard 1D NOESY pulse sequence. All 1D ^{1}H NMR spectra using a spectral width of 6009.6 Hz, and 128 transients collected with 16,384 data points (Liu et al., 2011). All the ^{1}H NMR spectra were generalized log transformed using transformation parameter $\lambda = 2 \times 10^{-8}$ (Parsons et al., 2007).

Multivariate data analysis was performed using SIMCA-P$^+$ (V11.0, Umetric, Sweden). In this study, supervised partial least squares discriminant analysis (PLS-DA) and orthogonal projection to latent structure with discriminant analysis (O-PLS-DA) were sequentially performed to reveal the statistically significant metabolite responses induced by BaP exposures.

The results were visualized in terms of scores plotted to show the classifications and corresponding loadings plots of the NMR spectral variables contributing to the classifications. The model coefficients were calculated from the coefficients incorporating the weight of the variables in order to enhance interpretability of the model. Then metabolic differences responsible for the classifications between solvent control groups, and BaP-exposed groups could be detected in the coefficient-coded loadings plots. The coefficient plots were generated by using Matlab (V7.0, the Math Works Inc., Natwick, USA) (Feng et al., 2013) and (Wu et al., 2013b).

2.3. Proteomics analysis of P. martensii gills

Total proteins in gills of *P. martensii* were extracted according to the modified procedure (Lee and Lo, 2008; Wu et al., 2013a). In brief, gills (~ 100 mg) were homogenized with 1 mL of TRIzol reagent to extract proteins at 4 °C. The protein pellets were dissolved in protein lysis buffer (7 M urea; 2 M thiourea; 4% m/V CHAPS; 65 mM DTT and 0.2% W/V Bio-lyte buffer) and incubated at 4 °C 4 until completely dissolved. The homogenate was centrifuged at 14,000 g for 30 min. The total concentration of proteins was determined by Bradford method (Bradford, 1976). Finally, the supernatant was applied to isoelectric focusing (IEF).

The two-dimensional gel electrophoresis (2-DE) technique was performed for proteomic analysis. The details were described previously by Chen et al. (2016). For the first dimension (isoelectric focusing, IEF), 1.2 mg of proteins in a final volume of 450 mL were loaded onto the Immobiline Drystrip (24 cm, pH 3–10, linear). The IEF was completed at 20 °C with an Ettan IPGphor3 system. The second dimension was performed on 12.5% SDS-PAGE gels using the Ettan DALTsix system. After the electrophoresis, proteins were stained by Coomassie brilliant blue (PhastGelTMBlue R, GE Healthcare) and were analyzed with ImageMaster 2D Platinum 7.0 software. For all the matched spots, only those protein spots with significant difference (Student's *t*-test, $p < 0.05$) of at least 1.5-fold were treated as differentially expressed.

Gel digestion was accomplished according to the procedure of Katayama et al. (2001). The completely dried samples were re-suspended with 5 mL of 0.1% trifluoroacetic acid subsequently mixed in 1:1 ratio with a saturated solution of acyano-4-hydroxy-trans-cinnamic acid in 50% acetonitrile. The peptides samples were analyzed, and mass spectra were obtained by MALDI-TOF/TOF mass spectrometer (ABI 4800, Applied Biosystems, USA). Data were acquired in a positive MS reflector using a CalMix5 standard to calibrate the instrument (ABI 4800 Calibration Mixture). Both the MS and MS/MS data were integrated and processed using the GPS Explorer V3.6 software (Applied Biosystems, USA) with default parameters. Proteins were successfully identified based on 95% or higher confidence interval of their scores in the MASCOT V2.4 search engine (Matrix Science Ltd., U.K.).

3. Results and discussion

3.1. Effects of BaP on metabolome of P. martensii gills

Fig. 1 shows a representative 1-dimensional 500 MHz ^{1}H NMR spectrum of *P. martensii* gill tissue extracts from the control group. Some major metabolites were detected in Fig. 1. They were classified as organic acids (fumarate, succinate and malonate), organic osmolytes (taurine, homarine, betaine, hypotaurine and dimethylglycine), amino acids (branched chain amino acid (BCAAs), alanine, tyrosine, glutamate, etc.), and energy storage compounds (glucose and ATP).

O-PLS-DA analysis indicated some significantly altered metabolites ($p < 0.05$) caused by exposure of gills to 10 μg/L BaP (Fig. 2, Table 1). Apparently, arginine, acetoacetate, malonate, and phosphocholine were

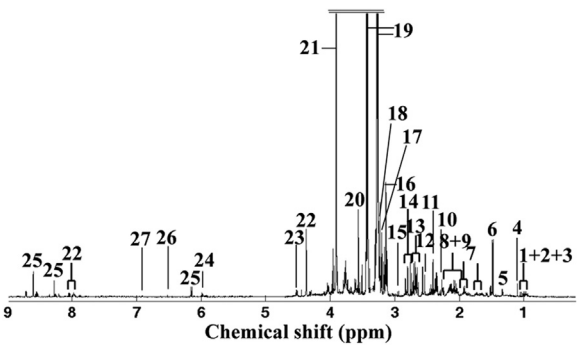

Fig. 1. A representative 1-dimensional 500 MHz ^{1}H NMR spectrum of gill tissue extract of *P. martensii* from the control group. **Keys**: 1. Isoleucine, 2. Leucine, 3. Valine, 4. Unknown 1 (1.10 ppm), 5. Threonine, 6. Alanine, 7. Arginine, 8. Glutamate, 9. Glutamine, 10. Acetoacetate, 11. Succinate, 12. β-alanine, 13. Hypotaurine, 14. Aspartate, 15. Dimethylglycine, 16. Malonate, 17. Choline, 18. Phosphocholine, 19. Taurine, 20. Glycine, 21. Betaine, 22. Homarine, 23. Glucose, 24. Unknown 2 (5.96 ppm), 25. ATP, 26. Fumarate and 27. Tyrosine.

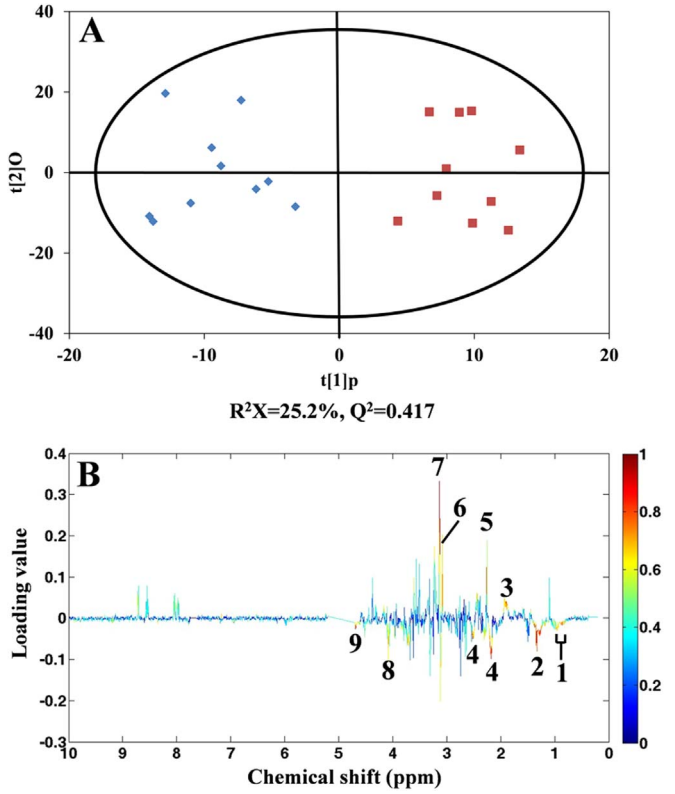

Fig. 2. OPLS-DA scores (A) derived from ^{1}H NMR spectra of gill tissue extracts from solvent control (◆) and 10 μg/L BaP-treated groups (■) and corresponding coefficient plot (B). The color map shows the significance of metabolite variations between the two classes (solvent control and BaP). Peaks in the positive direction indicate metabolites that are more abundant in the BaP-treated group. Consequently, metabolites that are more abundant in the control group are presented as peaks in the negative direction. **Keys**: 1. BCAAs (valine, leucine, and isoleucine), 2. Threonine, 3. Arginine, 4. Glutamine, 5. Acetoacetate, 6. Malonate, 7. Phosphocholine, 8. Unknown (4.10 ppm) and 9 Glucose. (For interpretation of the references to color in this figure legend, the reader is referred to the web version of this article.)

Table 1
Effects of 10 μg/L BaP exposure on differentially expressed metabolites in *P. martensii* gills.

Metabolites	Differentially expression ($p < 0.05$)[a]	
Arginine	↑	
Phosphocholine	↑	
Malonate	↑	
Acetoacetate	↑	
Glucose		↓
BCAAs		↓
Glutamine		↓
Threonine		↓

↑: Significantly up-regulated metabolites involved in various physiological functions.
↓: Significantly down-regulated metabolites involved in various physiological functions.
[a] p-Values determined using one-way ANOVA on the bin areas from the representative peak of the corresponding metabolite.

considerably increased. Conversely, BCAAs, threonine, glutamine and glucose were significantly decreased. However, 1 μg/L BaP did not induce a significant alteration in metabolites. This result is similar to previous research results (Ji et al., 2013; Chen et al., 2016). The sensitivity of NMR is comparatively lower than that of MS spectroscopy, and fewer than 50 metabolites were detected by NMR in the gill extracts (Fig. 1). As a result, the low abundance metabolic biomarkers may be neglected in the low dose BaP exposure group.

Arginine, phosphocholine, acetoacetate and malonate are involved in some energy metabolic pathways. Arginine is produced by the conversion of phosphoarginine (Viant et al., 2001). The concentration of arginine has been correlated to ATP/ADP (Fasulo et al., 2012). The increased arginine suggested that the disorder of energy metabolism of the urea cycle was induced by the high BaP concentration. Song et al. (2016a) reported 10 μg/L BaP and DDT affected arginine metabolism in green mussel *Perna viridis*. Phosphocholine is catalyzed by choline kinase, which converts choline and ATP into ADP and phosphocholine (Liu et al., 2014c). Thus, the elevated phosphocholine implied that reduced energy demand in *P. martensii* gills was induced by BaP. Such changes in phosphocholine may be associated with toxicant-induced oxidative stress, reactive oxygen species (ROS) production and lipid peroxidation, with potential alterations in cellular membrane stability (Brandão et al., 2015). Cappello et al. (2016a, 2016b) considered reduction in phosphocholine reflected the occurrence of membrane repair processes in gills of wild fish. In the present study, increased phosphocholine showed that BaP had strong cytotoxicity on gills of *P. martensii*, which affected membrane stabilization/repair process. Malonate competes with succinate and is a competitive inhibitor of cellular respiration, which is one key enzyme in the Krebs cycle (Zhang et al., 2011b). The increased malonate indicated that BaP is most likely to affect the Krebs cycle associated with energy metabolism in gills. Phosphocholine and malonate have shown the similar changes in *P. martensii* digestive glands exposed to 10 μg/L BaP (Chen et al., 2016). Acetoacetate is one kind of ketone body, and it is produced from acetyl-coenzyme A (acetyl-CoA) (Ji et al., 2015). The increased acetoacetate evinced that lipid metabolism was enhanced in gills exposed to high BaP concentration. Cappello et al. (2013) reported PAH pollution induced increased levels of acetoacetate and malonate in gills of mussels. These changes were associated with impairments in energy metabolism.

Evidently, the decline of BCAAs, glutamine, threonine, and glucose in gills was induced by the high BaP dose. BCAAs including leucine, isoleucine and valine can affect the immune system function by participating in the protein biosynthesis (Calder, 2006). Therefore, dramatically decreased BCAAs are one possible cause of immunological impairment in gills of *P. martensii*. Essentially, amino acids play significant roles in numerous biological pathways in marine mollusks. The altered glutamine and threonine might suggest that a disturbance in osmotic regulation of *P. martensii* gills was induced by the high BaP dose. However, some important organic osmolytes showed no significant change. According to a previous study, BaP induces osmotic regulation changes in *P. martensii* digestive glands (Chen et al., 2016). The reduced glucose in gills indicated a disorder in energy metabolism caused by exposure to 10 μg/L BaP. The changes of all these metabolites implied that the high BaP dose could induce disturbance in immune stress and disturb osmotic regulation and energy metabolism in *P. martensii* gills.

Previous research revealed that BaP induces a distinct metabolome in gills of different bivalves. At 10 μg/L, BaP primarily induces a disorder of osmotic regulation in *Perna viridis* (Song et al., 2016b). In the case of *Ruditapes philippinarum*, 50 μg/L BaP also disturbs the osmotic regulation and energy metabolism (Zhang et al., 2011b).

3.2. Effects of BaP on the proteome of *P. martensii* gills

Protein spots were compared between the solvent control and BaP treatment at two different concentrations; a total of thirteen proteins were significantly altered, including 5 down-regulated and 8 up-regulated proteins (Fig. 3). These proteins were principally involved in energy metabolism, signal transduction, transcription regulation, cell growth, and stress response. The details of all these proteins are described in Table 2.

The majority of proteins were evidently altered in the 10 μg/L BaP-treated group. N-terminal EF-hand calcium-binding protein 1, calmodulin and calumenin were detected, which are calcium binding proteins (CaBPs). CaBPs constitute a large family of proteins that participate in calcium cell signaling pathways by binding to Ca^{2+}. Calmodulin, a member of the EF-hand family of Ca^{2+}-sensing proteins, is a

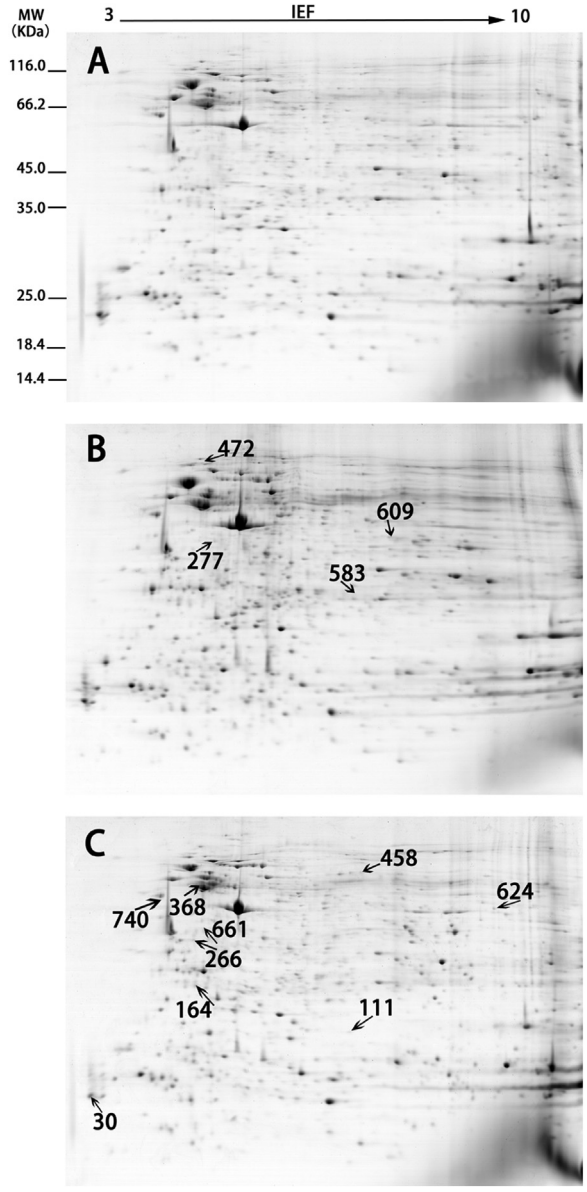

Fig. 3. Representative 2-DE images of proteins from gills of *P. martensii* exposed to different concentrations of BaP for 7 days. Proteins were submitted to IEF on 3–10 IPG strips (24 cm) followed by electrophoresis on 12.5% SDS-PAGE. Gels were stained with Coomassie brilliant blue. Gels (A, B, and C) are from the (A) solvent control, (B) 1 μg/L and (C) 10 μg/L BaP-treated groups. The proteins spots detected in all three biological replicates were analyzed by MALDI-TOF/TOF mass spectrometry and are described in Table 2.

prototypical calcium sensor (Chin and Means, 2000). Calumenin is found in the endoplasmic reticulum (ER) and carries a new ER retention signal (Yabe et al., 1997). Some studies have shown that this protein can bind to cystic fibrosis transmembrane conductance regulator CFTR and is likely involved in the regulated and mutated CFTR mutant protein (Teng et al., 2012; Tripathi et al., 2014). In this study, these abnormal proteins could indicate that the high BaP dose damaged the cellular Ca^{2+} homeostasis of gills.

As one structural protein, the variation in tubulin mean a cellular injury caused by physiological stress (Ji et al., 2013; Wu et al., 2013c). It is clear that the altered tubulin isoforms were.protein markers of cellular injury (Puerto et al., 2011). In our research, the up-regulated tubulin alpha-1C chain implies that 10 μg/L BaP induced a defense mechanism in gills. Activating signal cointegrator 1 (ASC-1) can be associated with specific components of the RNA polymerase II complex. As a co-activator of some nuclear receptors, it could play a major role in creating various co-activator complexes under different cellular conditions Some research demonstrated ASC-1 is a novel transcription coactivator molecule of nuclear receptors that participates in the transcription process (Kim et al., 1999; Jung et al., 2002). Activating signal cointegrator 1 complex subunit 1 is a part of the ASC-1 complex. High concentrations of BaP probably affected the transcription of *P. martensii* gills by affecting the expression of ASC-1 complex subunit 1. Heterogeneous nuclear ribonucleoprotein A/B (hnRNP A/B) regulates proteins associated with pathways related to DNA and RNA metabolism (He and Smith, 2009). The significant up-regulation of hnRNP A/B suggests a disturbance of nucleotide metabolism and nuclear processes in gills under the high concentration of BaP exposure.

Mitochondrial malate dehydrogenase (MDH2) and fructose-bisphosphate aldolase (FBA) are necessary enzymes in energy metabolism. MDH2 is involved in the malate metabolic process, which catalyzes the oxidation of malate to oxaloacetate (Minárik et al., 2002; Wei et al., 2015). FBA plays a vital role in the glycolytic process. In the present work, the up-regulation of MDH2 and the down-regulation of FBA perhaps suggests that the elevated BaP exposure interfered with the citrate cycle in *P. martensii* gills.

Some proteins were significantly altered in the 1 μg/L BaP-treated group. Guanine nucleotide-binding proteins play a vital role as a signal transducer in some processes such as organismal homeostasis and immune functions (Herroeder et al., 2009; Neves et al., 2002; Wu et al., 2013b). Serine/arginine (SR) proteins are essential pre-mRNA splicing factors and play numerous roles at the post-transcriptional level (Sanford et al., 2005). According to a new study of Moulton et al. (2015), serine-arginine-rich splicing factor 1 (SRSF1) contributes to transcriptional activation of CD3ζ in human T cells. The present research showed that the low dose BaP exposure could alter RNA processing to destroy the immune function of the gills. Cdc42 is a small GTPase of the Rho family that regulates signaling pathways that control various cellular functions including endocytosis, migration, cell cycle progression, and cell morphology (Kang et al., 2008; Pertz et al., 2008; Qadir et al., 2015).

Heat shock proteins (HSPs) constitute the major category of molecular chaperones indispensable for the maintenance of cellular functions (Hartl and Hayer-Hartl, 2002; Tsan and Gao, 2009). HSP90 is known to play a role in posttranslational regulation and protein folding. Mainly, it is involved in regulation of apoptosis (Sarto et al., 2000). The elevated levels of HSP90 show that 1 μg/L of BaP induced cellular immune responses in *P. martensii* gill cells. A similar response was obtained in the *P. martensii* digestive gland (Chen et al., 2016).

3.3. Comparative effects of BaP on metabolome and proteome of *P. martensii* gills

As shown in Fig. 4, alterations of metabolites and proteins involved in some metabolic pathways were induced by BaP exposure in gills according to Kyoto Encyclopedia of Genes and Genomes (http://www.genome.jp/kegg/) and UniProt (http://www.uniprot.org/). In the gills, there were many differential proteins involved in the signal transduction pathway, including N-terminal EF-hand calcium-binding protein 1, calmodulin, and calumenin were involved in the Ca^{+} signaling pathway. The primary metabolites involved in the citric acid cycle, urea cycle, and glycolysis had changed. Arginine, malonate, acetoacetate, and phosphocholine significantly increased, while BCAAs, glutamate and glucose significantly decreased.

The analysis revealed that certain differential proteins and metabolites participated in the same metabolic pathway. MDH2 and FBA were involved in malonate metabolism and glycolysis, respectively.

4. Conclusion

In summary, the toxic effects of BaP were mainly characterized by

Table 2
List of protein spots that were differentially expressed in *P. martensii* gills exposed to different concentrations of BaP (1 μg/L and 10 μg/L) for 7 days.

Spot ID[c]	Protein name	Species	Accession Number[d]	MW/kDa[e]	PI	Protein Score[f]	SC[g]	PN[h]	fold changes[i]
266	N-terminal EF-hand calcium-binding protein 1	Crassostrea gigas	gi|405978438	34,670	4.88	36	2%	1	6.13794[b]
164	Activating signal cointegrator 1 complex subunit 1	Crassostrea gigas	gi|405969929	41,363	5.58	36	2%	1	2.59801[b]
277	Guanine nucleotide-binding protein G(o) subunit alpha	Lymnaea stagnalis	gi|232136	40,759	5.24	138	9%	3	2.47455[a]
368	Tubulin alpha-1C chain	Crassostrea gigas	gi|405965637	50,794	4.94	739	23%	7	2.24416[b]
624	Malate dehydrogenase, mitochondrial	Crassostrea gigas	gi|524878971	37,839	7.03	78	3%	1	2.08846[b]
458	hypothetical protein LOTGIDRAFT_201713	Lottia gigantea	gi|556109516	50,749	4.90	44	3%	1	2.02419[b]
472	Heat shock protein 90	Crassostrea gigas	gi|558697274	83,289	4.88	615	17%	8	1.69803[a]
661	Heterogeneous nuclear ribonucleoprotein A/B	Crassostrea gigas	gi|405957004	23,918	5.15	68	13%	2	1.54752[b]
583	Splicing factor, arginine/serine-rich 1	Crassostrea gigas	gi|524874374	25,053	9.82	54	10%	2	− 7.74607[a]
609	Cdc42	Aplysia californica	gi|30385202	21,735	6.32	84	6%	1	− 5.44133[a]
30	Calmodulin	Aplysia californica	gi|21307641	16,800	4.09	193	30%	3	− 1.74469[b]
111	Fructose-bisphosphate aldolase	Anadara sp. KJP− 2011	gi|318136386	21,981	5.3	173	11%	1	− 1.68547[b]
740	Calumenin	Crassostrea gigas	gi|524910865	47,988	4.53	42	1%	1	− 1.6238[b]

[a] Identification of differentially expressed proteins compared with solvent control and BaP 1 μg/L.
[b] Identification of differentially expressed proteins compared with solvent control and BaP 10 μg/L.
[c] Assigned spot ID as indicated in Fig. 3.
[d] Database accession numbers after searching against the NCBInr database.
[e] Experimental mass.
[f] Mascot score reported.
[g] Sequence coverage.
[h] Number of peptide sequences.
[i] Fold changes with significances (> 1.5 folds and $p < 0.05$) were calculated using ImageMaster 2D Platinum 7.0.

abnormal metabolism of organic acids, disturbance of energy metabolism and alteration of signaling pathways in gills of the pearl oyster *P. martensii*. At the metabolite level, 10 μg/L BaP could induce harsher interference in energy metabolism, immune response and osmotic regulation via some abnormally altered metabolic biomarkers (arginine, acetoacetate, malonate and phosphocholine, BCAAs, threonine, glutamine, and glucose). Proteomic responses suggested that both 1 and 10 μg/L BaP induced disturbance of energy metabolism, signal transduction, transcription regulation, cell growth, and stress response via altered protein responses. These results indicated that metabolomic and proteomic were complementary, and the approaches could help better understand the underlying mechanism of toxicity of BaP exposure.

Acknowledgement

The research was funded by the National Natural Science Foundation of China (31160126 and 41161077). We thank the editors and the anonymous reviewers for their valuable comments and suggestions on the paper.

Conflicts of interest

The authors declare that there is no conflict of interests regarding the publication of this paper.

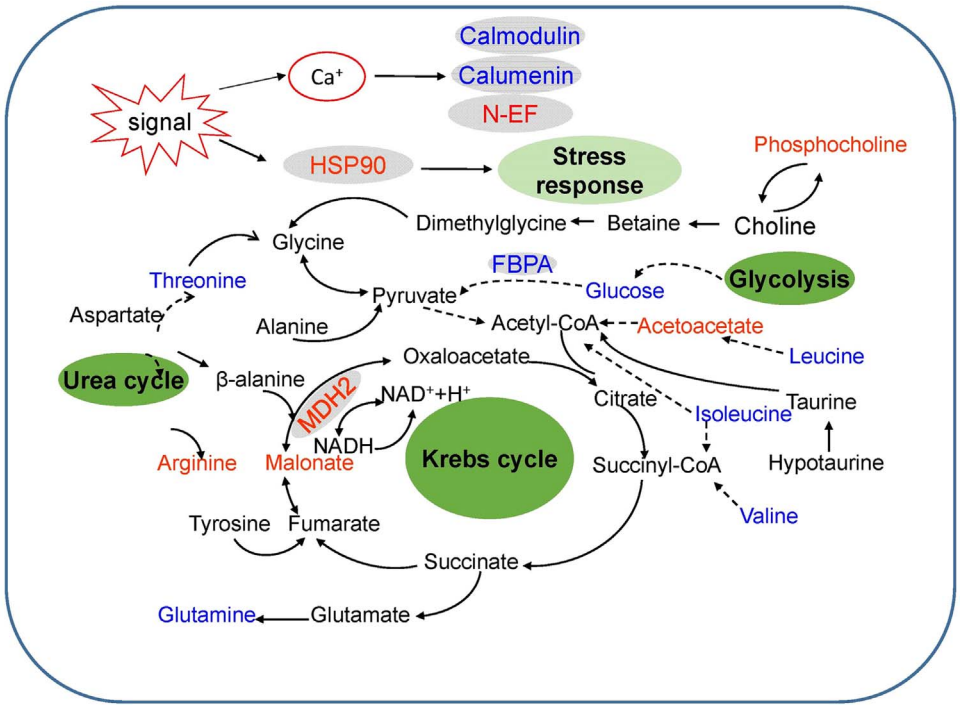

Fig. 4. A schematic presentation of pathways indicated by the altered metabolites and proteins induced by BaP in gills. The identified metabolites and proteins are shown by marking the names in red (up-regulated) or blue (down-regulated). Abbreviation: FBA, Fructose-bisphosphate aldolase; MDH2, mitochondrial malate dehydrogenase; HSP 90, Heat shock protein 90. (For interpretation of the references to color in this figure legend, the reader is referred to the web version of this article.)

References

Azevedo, C.C., Guzmán-Guillén, R., Martins, J.C., Osório, H., Vasconcelos, V., da Fonseca, R.R., Campos, A., 2015. Proteomic profiling of gill GSTs in *Mytilus galloprovincialis* from the North of Portugal and Galicia evidences variations at protein isoform level with a possible relation with water quality. Mar. Environ. Res. 110, 152–161.

Bradford, M.M., 1976. A rapid and sensitive method for the quantitation of microgram quantities of protein utilizing the principle of protein-dye binding. Anal. Biochem. 72, 248–254.

Brandão, F., Cappello, T., Raimundo, J., Santos, M.A., Maisano, M., Mauceri, A., Pacheco, M., Pereira, P., 2015. Unravelling the mechanisms of mercury hepatotoxicity in wild fish (*Liza aurata*) through a triad approach: bioaccumulation, metabolomic profiles and oxidative stress. Metallomics 7, 1352–1363.

Braz-Mota, S., Sadauskas-Henrique, H., Duarte, R.M., Val, A.L., Almeida-Val, V.M., 2015. Roundup(R) exposure promotes gills and liver impairments, DNA damage and inhibition of brain cholinergic activity in the Amazon teleost fish *Colossoma macropomum*. Chemosphere 135, 53–60.

Calder, P.C., 2006. Branched-chain amino acids and immunity. J. Nutr. 136, 288S–293S.

Campos, A., Tedesco, S., Vasconcelos, V., Cristobal, S., 2012. Proteomic research in bivalves: towards the identification of molecular markers of aquatic pollution. J. Proteom. 75, 4346–4359.

Cappello, T., Pereira, P., Maisano, M., Mauceri, A., Pacheco, M., Fasulo, S., 2016a. Advances in understanding the mechanisms of mercury toxicity in wild golden grey mullet (*Liza aurata*) by ^{1}H NMR-based metabolomics. Environ. Pollut. 219, 139–148.

Cappello, T., Mauceri, A., Corsaro, C., Maisano, M., Parrino, V., Lo Paro, G., Messina, G., Fasulo, S., 2013. Impact of environmental pollution on caged mussels *Mytilus galloprovincialis* using NMR-based metabolomics. Mar. Pollut. Bull. 77, 132–139.

Cappello, T., Brandao, F., Guilherme, S., Santos, M.A., Maisano, M., Mauceri, A., Canario, J., Pacheco, M., Pereira, P., 2016b. Insights into the mechanisms underlying mercury-induced oxidative stress in gills of wild fish (*Liza aurata*) combining (1)H NMR metabolomics and conventional biochemical assays. Sci. Total Environ. 548–549, 13–24.

Chen, H., Song, Q., Diao, X., Zhou, H., 2016. Proteomic and metabolomic analysis on the toxicological effects of Benzo[a]pyrene in pearl oyster *Pinctada martensii*. Aquat. Toxicol. 175, 81–89.

Chin, D., Means, A.R., 2000. Calmodulin: a prototypical calcium sensor. Trends Cell. Biol. 10, 322–328.

Chivittz, C.C., Pinto, D.P., Ferreira, R.S., Sopezki Mda, S., Fillmann, G., Zanette, J., 2016. Responses of the CYP1A biomarker in *Jenynsia multidentata* and *Phalloceros caudimaculatus* and evaluation of a CYP1A refractory phenotype. Chemosphere 144, 925–931.

Ciacci, C., Barmo, C., Gallo, G., Maisano, M., Cappello, T., D'Agata, A., Leonzio, C., Mauceri, A., Fasulo, S., Canesi, L., 2012. Effects of sublethal, environmentally relevant concentrations of hexavalent chromium in the gills of *Mytilus galloprovincialis*. Aquat. Toxicol. 120–121, 109–118.

Corrales, J., Thornton, C., White, M., Willett, K.L., 2014. Multigenerational effects of benzo[a]pyrene exposure on survival and developmental deformities in zebrafish larvae. Aquat. Toxicol. 148, 16–26.

Costa, P.M., Chicano-Galvez, E., Lopez Barea, J., DelValls, T.A., Costa, M.H., 2010. Alterations to proteome and tissue recovery responses in fish liver caused by a short-term combination treatment with cadmium and benzo[a]pyrene. Environ. Pollut. 158, 3338–3346.

D'Agata, A., Cappello, T., Maisano, M., Parrino, V., Giannetto, A., Brundo, M.V., Ferrante, M., Mauceri, A., 2014. Cellular biomarkers in the mussel *Mytilus galloprovincialis* (Bivalvia: Mytilidae) from Lake Faro (Sicily, Italy). Ital. J. Zool. 81, 43–54.

Du, J., Liao, C., Zhou, H., Diao, X., Li, Y., Zheng, P., Wang, F., 2015. Gene cloning and expression analysis of AhR and CYP4 from *Pinctada martensii* after exposed to pyrene. Ecotoxicology 24, 1574–1582.

Fasulo, S., Iacono, F., Cappello, T., Corsaro, C., Maisano, M., D'Agata, A., Giannetto, A., De Domenico, E., Parrino, V., Lo Paro, G., Mauceri, A., 2012. Metabolomic investigation of *Mytilus galloprovincialis* (Lamarck 1819) caged in aquatic environments. Ecotoxicol. Environ. Saf. 84, 139–146.

Feng, J., Li, J., Wu, H., Chen, Z., 2013. Metabolic responses of HeLa cells to silica nanoparticles by NMR-based metabolomic analyses. Metabolomics 9, 874–886.

Hartl, F.U., Hayer-Hartl, M., 2002. Molecular chaperones in the cytosol: from nascent chain to folded protein. Science 295, 1852–1858.

He, Y., Smith, R., 2009. Nuclear functions of heterogeneous nuclear ribonucleoproteins A/B. Cell. Mol. Life Sci.: CMLS 66, 1239–1256.

Herroeder, S., Reichardt, P., Sassmann, A., Zimmermann, B., Jaeneke, D., Hoeckner, J., Hollmann, M.W., Fischer, K.D., Vogt, S., Grosse, R., Hogg, N., Gunzer, M., Offermanns, S., Wettschureck, N., 2009. Guanine nucleotide-binding proteins of the G12 family shape immune functions by controlling CD4+ T cell adhesiveness and motility. Immunity 30, 708–720.

Ji, C., Li, F., Wang, Q., Zhao, J., Sun, Z., Wu, H., 2016. An integrated proteomic and metabolomic study on the gender-specific responses of mussels *Mytilus galloprovincialis* to tetrabromobisphenol A (TBBPA). Chemosphere 144, 527–539.

Ji, C., Wang, Q., Wu, H., Tan, Q., Wang, W.X., 2015. A metabolomic investigation of the effects of metal pollution in oysters *Crassostrea hongkongensis*. Mar. Pollut. Bull. 90, 317–322.

Ji, C., Wu, H., Wei, L., Zhao, J., Yu, J., 2013. Proteomic and metabolomic analysis reveal gender-specific responses of mussel *Mytilus galloprovincialis* to 2,2',4,4'-tetrabromodiphenyl ether (BDE 47). Aquat. Toxicol. 140–141, 449–457.

Jung, D.J., Sung, H.S., Goo, Y.W., Lee, H.M., Park, O.K., Jung, S.Y., Lim, J., Kim, H.J., Lee, S.K., Kim, T.S., Lee, J.W., Lee, Y.C., 2002. Novel transcription coactivator complex containing activating signal cointegrator 1. Mol. Cell. Biol. 22, 5203–5211.

Kang, R., Wan, J., Arstikaitis, P., Takahashi, H., Huang, K., Bailey, A.O., Thompson, J.X., Roth, A.F., Drisdel, R.C., Mastro, R., Green, W.N., Yates, J.R., Davis, N.G., El-Husseini, A., 2008. Neural palmitoyl-proteomics reveals dynamic synaptic palmitoylation. Nature 456, 904–909.

Karim, M., Puiseux-Dao, S., Edery, M., 2011. Toxins and stress in fish: proteomic analyses and response network. Toxicon 57, 959–969.

Katayama, H., Nagasu, T., Oda, Y., 2001. Improvement of in-gel digestion protocol for peptide mass fingerprinting by matrix-assisted laser desorption/ionization time-of-flight mass spectrometry. Rapid Commun. Mass Sp. 15, 1416–1421.

Kim, H.-J., Yi, J.-Y., Sung, H.-S., Moore, D.D., Jhun, B.H., Lee, Y.C., Lee, J.W., 1999. Activating signal cointegrator 1, a novel transcription coactivator of nuclear receptors, and its cytosolic localization under conditions of serum deprivation. Mol. Cell. Biol. 19, 6323–6332.

Lee, F.W., Lo, S.C., 2008. The use of Trizol reagent (phenol/guanidine isothiocyanate) for producing high quality two-dimensional gel electrophoretograms (2-DE) of dinoflagellates. J. Microbiol Methods 73, 26–32.

Lin, C.Y., Wu, H., Tjeerdema, R.S., Viant, M.R., 2007. Evaluation of metabolite extraction strategies from tissue samples using NMR metabolomics. Metabolomics 3, 55–67.

Liu, N., Pan, L., Gong, X., Tao, Y., Hu, Y., Miao, J., 2014a. Effects of benzo(a)pyrene on differentially expressed genes and haemocyte parameters of the clam *Venerupis philippinarum*. Ecotoxicology 23, 122–132.

Liu, D., Pan, L., Cai, Y., Li, Z., Miao, J., 2014b. Response of detoxification gene mRNA expression and selection of molecular biomarkers in the clam *Ruditapes philippinarum* exposed to benzo[a]pyrene. Environ. Pollut. 189, 1–8.

Liu, X., Ji, C., Zhao, J., Wang, Q., Li, F., Wu, H., 2014c. Metabolic profiling of the tissue-specific responses in mussel *Mytilus galloprovincialis* towards Vibrio harveyi challenge. Fish Shellfish Immunol. 39, 372–377.

Liu, X., Zhang, L., You, L., Yu, J., Cong, M., Wang, Q., Li, F., Li, L., Zhao, J., Li, C., Wu, H., 2011. Assessment of Clam *Ruditapes philippinarum* as heavy metal bioindicators using NMR-based metabolomics. Clean - Soil Air Water 39, 759–766.

Maria, V.L., Gomes, T., Barreira, L., Bebianno, M.J., 2013. Impact of benzo(a)pyrene, Cu and their mixture on the proteomic response of *Mytilus galloprovincialis*. Aquat. Toxicol. 144–145, 284–295.

Minárik, P., Tomásková, N., Kollárová, M., Antalík, M., 2002. Malate dehydrogenases-structure and function. Gen. Physiol. Biophys. 21, 257–265.

Moulton, V.R., Gillooly, A.R., Perl, M.A., Markopoulou, A., Tsokos, G.C., 2015. Serine arginine-rich splicing factor 1 (SRSF1) contributes to the transcriptional activation of CD3ζ in human T cells. PLoS One 10, e0131073.

Neves, S.R., Ram, P.T., Iyengar, R., 2002. G protein pathways. Science 296, 1636–1639.

Panfoli, I., Burlando, B., Viarengo, A., 2000. Effects of heavy metals on phospholipase C in gill and digestive gland of the marine mussel *Mytilus galloprovincialis* Lam. Comp. Biochem. Physiol. B Biochem. Mol. Biol. 127, 391–397.

Parsons, H.M., Ludwig, C., Gunther, U.L., Viant, M.R., 2007. Improved classification accuracy in 1- and 2-dimensional NMR metabolomics data using the variance stabilising generalised logarithm transformation. BMC Bioinforma. 8, 234.

Pertz, O.C., Wang, Y., Yang, F., Wang, W., Gay, L.J., Gristenko, M.A., Clauss, T.R., Anderson, D.J., Liu, T., Auberry, K.J., Camp, D.G., Smith, R.D., Klemke, R.L., 2008. Spatial mapping of the neurite and soma proteomes reveals a functional Cdc42/Rac regulatory network. Proc. Natl. Acad. Sci. USA 105, 1931–1936.

Phillips, D.H., 1999. Polycyclic aromatic hydrocarbons in the diet. Mutat. Res. 443, 139–147.

Puerto, M., Campos, A., Prieto, A., Camean, A., de Almeida, A.M., Coelho, A.V., Vasconcelos, V., 2011. Differential protein expression in two bivalve species; *Mytilus galloprovincialis* and *Corbicula fluminea*; exposed to Cylindrospermopsis raciborskii cells. Aquat. Toxicol. 101, 109–116.

Qadir, M.I., Parveen, A., Ali, M., 2015. Cdc42: role in cancer management. Chem. Biol. Drug Des. 86, 432–439.

Qiu, Y.-W., Zhang, G., Liu, G.-Q., Guo, L.-L., Li, X.-D., Wai, O., 2009. Polycyclic aromatic hydrocarbons (PAHs) in the water column and sediment core of Deep Bay, South China. Estuar. Coast. Shelf Sci. 83, 60–66.

Rust, A.J., Burgess, R.M., Brownawell, B.J., McElroy, A.E., 2004. Relationship between metabolism and bioaccumulation of benzo [α] pyrene in benthic invertebrates. Environ. Toxicol. Chem. 23 (11), 2587–2593.

Sanford, J.R., Ellis, J., Ca´ceres, J.F., 2005. Multiple roles of arginine/serine-rich splicing factors in RNA processing. Biochem. Soc. Trans. 33, 443–446.

Santacroce, M.P., Pastore, A.S., Tinelli, A., Colamonaco, M., Crescenzo, G., 2015. Implications for chronic toxicity of benzo[a]pyrene in sea bream cultured hepatocytes: cytotoxicity, inflammation, and cancerogenesis. Environ. Toxicol. 30, 1045–1062.

Sarto, C., Binz, P.A., Mocarelli, P., 2000. Heat shock proteins in human cancer. Electrophoresis 21, 1218–1226.

Shi, Y., Yu, C., Gu, Z., Zhan, X., Wang, Y., Wang, A., 2013. Characterization of the pearl oyster (*Pinctada martensii*) mantle transcriptome unravels biomineralization genes. Mar. Biotechnol. 15, 175–187.

Slattery, M., Ankisetty, S., Corrales, J., Marsh-Hunkin, K.E., Gochfeld, D.J., Willett, K.L., Rimoldi, J.M., 2012. Marine proteomics: a critical assessment of an emerging technology. J. Nat. Prod. 75, 1833–1877.

Song, Q., Zheng, P., Qiu, L., Jiang, X., Zhao, H., Zhou, H., Han, Q., Diao, X., 2016a. Toxic effects of male Perna viridis gonad exposed to BaP, DDT and their mixture: a metabolomic and proteomic study of the underlying mechanism. Toxicol. Lett. 240 (1), 185–195.

Song, Q., Chen, H., Li, Y., Zhou, H., Han, Q., Diao, X., 2016b. Toxicological effects of benzo(a)pyrene, DDT and their mixture on the green mussel *Perna viridis* revealed by proteomic and metabolomic approaches. Chemosphere 144, 214–224.

Teng, L., Kerbiriou, M., Taiya, M., Le Hir, S., Mignen, O., Benz, N., Trouve, P., Ferec, C., 2012. Proteomic identification of calumenin as a G551D-CFTR associated protein. PLoS One 7, e40173.

Tian, S., Pan, L., Tao, Y., Sun, X., 2015. Environmentally relevant concentrations of benzo [a]pyrene affect steroid levels and affect gonad of male scallop *Chlamys farreri*. Ecotoxicol. Environ. Saf. 114, 150–156.
Tikunov, A.P., Johnson, C.B., Lee, H., Stoskopf, M.K., Macdonald, J.M., 2010. Metabolomic investigations of American oysters using H NMR spectroscopy. Mar. Drugs 8, 2578–2596.
Tomanek, L., 2014. Proteomics to study adaptations in marine organisms to environmental stress. J. Proteom. 105, 92–106.
Tripathi, R., Benz, N., Culleton, B., Trouve, P., Ferec, C., 2014. Biophysical characterisation of calumenin as a charged F508del-CFTR folding modulator. PLoS One 9, e104970.
Tsan, M.F., Gao, B., 2009. Heat shock proteins and immune system. J. Leukoc. Biol. 85, 905–910.
Tung, E.W., Philbrook, N.A., Belanger, C.L., Ansari, S., Winn, L.M., 2014. Benzo[a]pyrene increases DNA double strand break repair in vitro and in vivo: a possible mechanism for benzo[a]pyrene-induced toxicity. Mutat. Res.-Genet. Toxicol. Environ. 760, 64–69.
Uno, S., Sakurai, K., Nebert, D.W., Makishima, M., 2014. Protective role of cytochrome P450 1A1 (CYP1A1) against benzo[a]pyrene-induced toxicity in mouse aorta. Toxicology 316, 34–42.
Valavanidis, A., Vlachogianni, T., Triantafillaki, S., Dassenakis, M., Androutsos, F., Scoullos, M., 2008. Polycyclic aromatic hydrocarbons in surface seawater and in indigenous mussels (*Mytilus galloprovincialis*) from coastal areas of the Saronikos Gulf (Greece). Estuar. Coast. Shelf Sci. 79, 733–739.
Van Hummelen, P., Sasaki, J., 2010. State-of-the-art genomics approaches in toxicology. Mutat. Res. 705, 165–171.
Viant, M.R., Rosenblum, E.S., Tjeerdema, R.S., 2001. Optimized method for the determination of phosphoarginine in abalone tissue by high-performance liquid chromatography. J. Chromatogr. 765, 107–111.
Viant, M.R., Rosenblum, E.S., Tjeerdema, R.S., 2003. NMR-based metabolomics: a powerful approach for characterizing the effects of environmental stressors on organism health. Environ. Sci. Technol. 37, 4982–4989.
Wei, L., Wang, Q., Ning, X., Mu, C., Wang, C., Cao, R., Wu, H., Cong, M., Li, F., Ji, C., Zhao, J., 2015. Combined metabolome and proteome analysis of the mantle tissue from Pacific oyster *Crassostrea gigas* exposed to elevated pCO2. Comp. Biochem. Physiol. Part D Genom. Proteom. 13, 16–23.
Williams, R., Hubberstey, A.V., 2014. Benzo(a)pyrene exposure causes adaptive changes in p53 and CYP1A gene expression in Brown bullhead (*Ameiurus nebulosus*). Aquat. Toxicol. 156, 201–210.
Wills, L.P., Jung, D., Koehrn, K., Zhu, S., Willett, K.L., Hinton, D.E., Di Giulio, R.T., 2010. Comparative chronic liver toxicity of benzo[a]pyrene in two populations of the atlantic killifish (*Fundulus heteroclitus*) with different exposure histories. Environ. Health Perspect. 118, 1376–1381.
Wu, H., Ji, C., Wei, L., Zhao, J., 2013a. Evaluation of protein extraction protocols for 2DE in marine ecotoxicoproteomics. Proteomics 13, 3205–3210.
Wu, H., Ji, C., Wei, L., Zhao, J., Lu, H., 2013b. Proteomic and metabolomic responses in hepatopancreas of *Mytilus galloprovincialis* challenged by Micrococcus luteus and Vibrio anguillarum. J. Proteom. 94, 54–67.
Wu, H., Liu, X., Zhang, X., Ji, C., Zhao, J., Yu, J., 2013c. Proteomic and metabolomic responses of clam *Ruditapes philippinarum* to arsenic exposure under different salinities. Aquat. Toxicol. 136–137, 91–100.
Wu, H., Southam, A.D., Hines, A., Viant, M.R., 2008. High-throughput tissue extraction protocol for NMR- and MS-based metabolomics. Anal. Biochem. 372, 204–212.
Wu, H., Wang, W.X., 2010. NMR-based metabolomic studies on the toxicological effects of cadmium and copper on green mussels *Perna viridis*. Aquat. Toxicol. 100, 339–345.
Yabe, D., Nakamura, T., Kanazawa, N., Tashiro, K., Honjo, T., 1997. Calumenin, a Ca21-binding protein retained in the endoplasmic reticulum with a novel carboxyl-terminal sequence, HDEF. J. Biol. Chem. 272, 18232–18239.
Yu, D., Ji, C., Zhao, J., Wu, H., 2016. Proteomic and metabolomic analysis on the toxicological effects of As (III) and As (V) in juvenile mussel *Mytilus galloprovincialis*. Chemosphere 150, 194–201.
Zena, R., Speciale, A., Calabro, C., Calo, M., Palombieri, D., Saija, A., Cimino, F., Trombetta, D., Lo Cascio, P., 2015. Exposure of sea bream (*Sparus aurata*) to toxic concentrations of benzo[a]pyrene: possible human health effect. Ecotoxicol. Environ. Saf. 122, 116–125.
Zhang, L., Liu, X., You, L., Zhou, D., Wu, H., Li, L., Zhao, J., Feng, J., Yu, J., 2011a. Metabolic responses in gills of Manila clam *Ruditapes philippinarum* exposed to copper using NMR-based metabolomics. Mar. Environ. Res. 72, 33–39.
Zhang, L., Liu, X., You, L., Zhou, D., Wang, Q., Li, F., Cong, M., Li, L., Zhao, J., Liu, D., Yu, J., Wu, H., 2011b. Benzo(a)pyrene-induced metabolic responses in Manila clam *Ruditapes philippinarum* by proton nuclear magnetic resonance ((1)H NMR) based metabolomics. Environ. Toxicol. Pharmacol. 32, 218–225.
Zhang, Z.L., Hong, H.S., Zhou, J.L., Yu, G., 2004. Phase association of polycyclic aromatic hydrocarbons in the Minjiang River Estuary, China. Sci. Total Environ. 323, 71–86.
Zhao, Y., Luo, K., Fan, Z., Huang, C., Hu, J., 2013. Modulation of benzo[a]pyrene-induced toxic effects in Japanese medaka (*Oryzias latipes*) by 2,2',4,4'-tetrabromodiphenyl ether. Environ. Sci. Technol. 47, 13068–13076.